ELSEVIER

Journal of Chromatography A, 698 (1995) 89–105

JOURNAL OF CHROMATOGRAPHY A

Review

Advances in affinity electrophoresis

Kazusuke Takeo

Yamaguchi Prefectural Public Health and Nursing College, Izumi-machi 21-1, Hofu-shi, 747, Japan

Abstract

Affinity electrophoresis is a technique with which macromolecules such as proteins and nucleic acids can be separated and characterized according to their biospecific interactions. In 1972, the first quantitative application of affinity electrophoresis was reported in the study of the phosphorylase–glycogen interaction. Microheterogeneity of serum glycoproteins was identified with the use of the carbohydrate-binding specificity of lectins. In the following years, various biospecific interactions were studied and characterized by affinity electrophoresis, and affinity electrophoresis has now become a general biochemical technique for analysing biospecific interactions, complementary to affinity chromatography. The resolving power of affinity electrophoresis is high. The technique is convenient for calculating thermodynamic parameters of biospecific interactions. As in the case of induced anti-hapten antibodies, affinity differences as small as 5% in the dissociation constant can be differentiated by the use of two-dimensional affinity electrophoresis. The high resolving power of the recently developed capillary gel affinity electrophoresis with an automatic operation system offers a powerful tool to analyse biospecific interactions.

Contents

0021-9673/95/$29.00
SSDI 0021-9673(94)01265-2

1. Introduction

Affinity electrophoresis (AEP) [1] is a technique by which the molecular properties of biological macromolecules such as proteins and nucleic acids are characterized and their specific interactions with corresponding affinity ligands are analysed. When glycogen phosphorylase is subjected to polyacrylamide gel disc electrophoresis in the presence of glycogen in the separating gel, its electrophoretic migration distance will decrease. This mobility change of phosphorylase is specific for glycogen and the extent of the mobility change is dependent on glycogen concentration. Based on the principle of enzyme kinetics using the mobility change of phosphorylase as a function of glycogen concentration, Takeo and Nakamura [2] derived an affinity equation and calculated with it the dissociation constants (K_d^{app}) of phosphorylases of rabbit skeletal muscle, liver and brain for glycogen. The values obtained coincided well with those obtained from enzyme kinetics [3]. This study was the first application of electrophoresis to the kinetic analysis of biospecific interactions.

The mobility change of phosphorylase by glycogen was cancelled when an oligosaccharide of α-(1→4)-D-glucan, such as maltotriose or cyclodextrin, is added to the gel [4]. These maltose oligosaccharides compete with glycogen for binding at the glycogen binding site of the enzyme. Based on the principle of inhibition kinetics using the mobility change of phosphorylase as a function of oligosaccharide concentration in the presence of a constant concentration of glycogen, dissociation constants (K_i) of phosphorylase–oligosaccharide interaction were calculated.

The term "affinity electrophoresis" was first proposed by Bøg-Hansen [5] and used by Hořejší and Kocourek [6] and Caron et al. [7]. Every electrophoretic process which explores biospecific interactions falls into the category of affinity electrophoresis. It includes cross-electrophoresis [8], crossed affinity immunoelectrophoresis [5], affinity electrophoretic titration [9], lectin affinity electrophoresis [10,11] and others. There are general reviews of affinity electrophoresis [1,12,13] and affinity electrophoresis of glycoproteins [14,15]. Because of limited space, this review briefly describes the basic principles of affinity electrophoresis and quantitative affinity electrophoresis with the latest applications, especially the thermodynamic analysis of biospecific interactions by affinity electrophoresis, and the development of two-dimensional affinity electrophoresis for the elucidation of antibody heterogeneity, lectin affinity electrophoresis for characterizing glycoprotein and newly developed capillary gel affinity electrophoresis.

2. Basic principle of affinity electrophoresis

2.1. Calculation of apparent dissociation constant

Kinetic constants are dependent on temperature. Well controlled thermostated electrophoresis apparatus [16] should be utilized. The apparent dissociation constant (K_d^{app}) is calculated by the following equation [17]:

$$1/(R_0 - r) = 1/(R_0 - R_c)[1 + (K_d^{app}/c)] \quad (1)$$

where R_0, r and R_c are the relative migration distances of protein in the absence and in the presence of an affinity ligand at concentration c and in the presence of an excess amount of affinity ligand, so that all the protein forms a complex with the affinity ligand. When Eq. 1 is plotted with $1/(R_0 - r)$ on the ordinate and $1/c$ on the abscissa, a straight line is obtained. The intercept of the line on the abscissa gives the negative reciprocal apparent dissociation constant ($-1/K_d^{app}$), and from the intercept on the ordinate, R_c can be calculated.

In practice, one set of electrophoresis is generally performed with twelve tubes [16], for which two separating gels are prepared in the absence of the affinity ligand and the other ten in the presence of five different concentrations of the affinity ligand in duplicate. The affinity ligand is added to the separating gel at a uniform concentration throughout the gels. The polyacrylamide concentration in the separating gel is

dependent on the magnitude of the molecular sieve effect of the gel on the sample protein. After electrophoresis, the gels are removed from the glass tubes and stained by protein staining or by activity staining. R_0 and r are calibrated with every gel. In Fig. 1, the affinity electrophoresis pattern of the concanavalin A–dextran T-2000 (average molecular mass $M_r = 2 \cdot 10^6$) interaction [16] is presented.

Eq. 1 is valid not only for the interaction between a protein and a macromolecule such as Dextran T-2000 ($M_r = 2 \cdot 10^6$) [16] or glycogen ($M_r > 1 \cdot 10^6$) [2,23] in polyacyrlamide gel, where the mobility of the complex is zero ($R_c = 0$), because of the complete molecular effect of the gel, but also for interactions where the mobilities of the free protein (R_0) and its complex with an affinity ligand (R_c) are different, because of the partial molecular sieve effect, as in the case of the interaction between concanavalin A and Dextran T-40 (M_r $4 \cdot 10^4$) in polyacrylamide gel [12], or because of the charge difference between the sample protein and its complex, as in the case of the interaction between serum glycoprotein and concanavalin A in agarose gel [17]. Bøg-Hansen and Takeo [17] calculated the apparent dissociation constants of various human serum glycoproteins for concanavalin A and Heegaard and Bjerrum [18] of anti-human serum albumin monoclonal antibody and anti-human α-fetoprotein monoclonal antibody for the corresponding antigens with Eq. 1 in crossed affinity immunoelectrophoresis. Eq. 1 has been designated the general affinity equation [1].

When $R_c = 0$, as in the case of the phosphorylase–glycogen or the concanavalin A–dextran T-2000 interaction, Eq. 1 is simplified to

$$1/r = 1/R_0[1 + (c/K_d^{app})] \quad (2)$$

When Eq. 2 is plotted with $1/r$ on the ordinate and c on the abscissa, a straight line is obtained. The intercept of the line on the abscissa gives the negative apparent dissociation constant ($-K_d^{app}$). In Fig. 2, affinity plots obtained with Eq. 2 for the concanavlin A–dextran T-2000 interaction at various temperatures [16] are illustrated. Each plot gives a straight line, verifying the theory. Eq. 2 has been designated the original affinity equation [1].

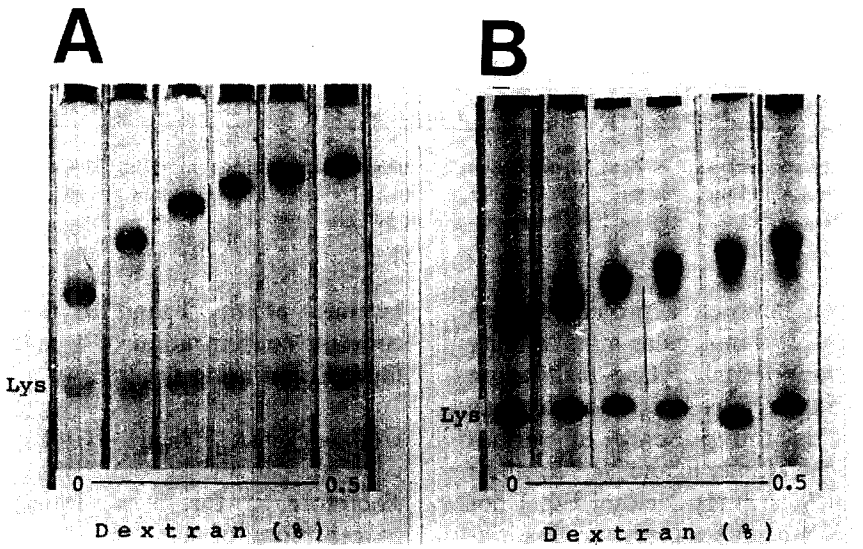

Fig. 1. Effect of temperature on affinity pattern of interaction between concanavalin A and dextran (from Ref. [16]). Electrophoresis was carried out in a 5% polyacrylamide gel containing 0, 0.1, 0.2, 0.3, 0.4 and 0.5% Dextran T-2000 at (A) 22°C and (B) 50°C. Lys (egg white lysosyme band) is used as the reference protein to calculate the relative migration distance.

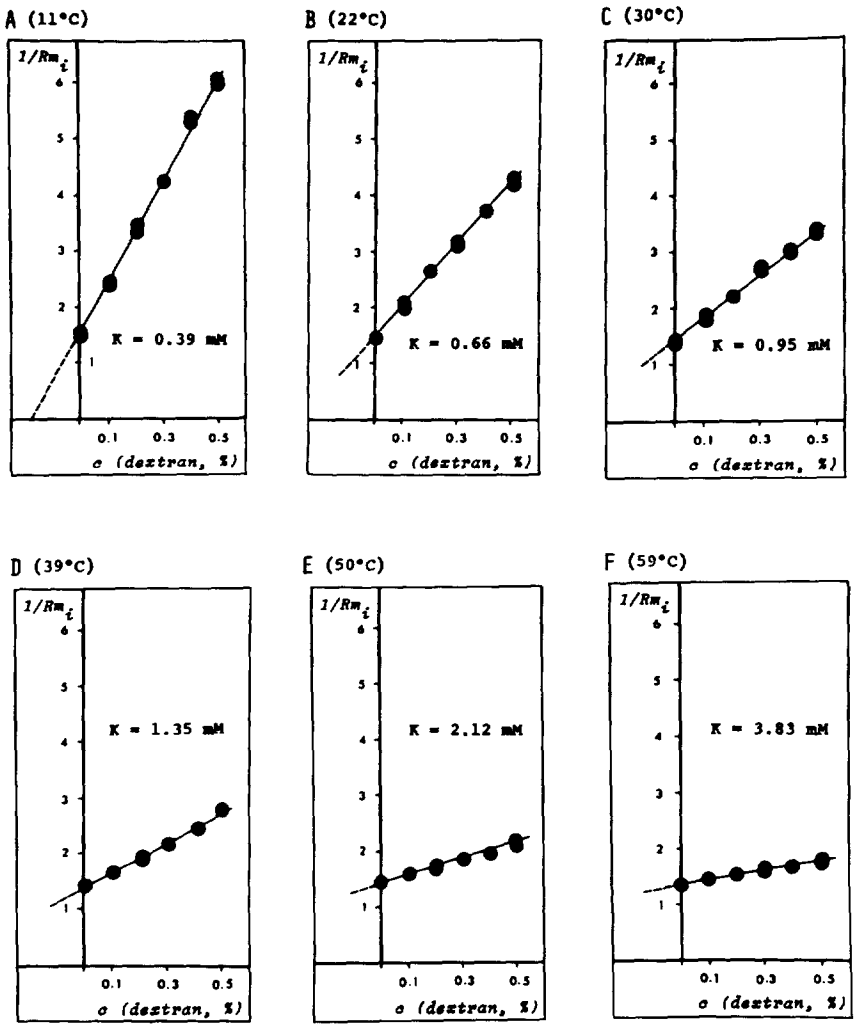

Fig. 2. Affinity plots of concanavalin A–dextran interaction at various temperatures (from Ref. [16]). The plots were drawn according to Eq. 2. The scale of the ordinate, $1/Rm_i$, should be read as $1/r$ here. K_d^{app}: 0.39 mM at 11°C, 0.66 mM at 22°C, 0.95 mM at 30°C, 1.35 mM at 39°C, 2.12 mM at 50°C and 3.83 mM at 59°C.

In an interaction between a protein and an electrically neutral low-molecular-mass affinity ligand, such as the phosphorylase–maltotriose interaction, where the relative migration distance remains constant in the presence of various concentrations of the affinity ligand, R_c, R_0 and r are identical ($R_c = R_0 = r$) [1]. Neither Eq. 1 nor Eq. 2 is applicable. In such a case, the dissociation constant can be calculated [4] by computing the recovery rate of the relative migration distance at various concentrations of a low-molecular-mass affinity ligand in the presence of a constant concentration of a macromolecular affinity ligand using the following equation:

$$r/(R_0 - r) = (K_d^{app}/c_0)[1 + (i/K_i)] \quad (3)$$

Therefore, if Eq. 3 is plotted at a constant concentration of glycogen, c_0, with $r/(R_0 - r)$ on the ordinate and various concentrations of maltotriose, i, on the abscissa, a straight line is obtained. The intercept of the line on the abscis-

sa gives the negative apparent dissociation constant for maltotriose ($-K_i$). Eq. 3 has been assignated the inhibition affinity equation [1].

2.2. Calculation of thermodynamic parameters

Thermodynamic parameters are calculated using the following equations:

$$\Delta G^0 = 2.303RT \log K_d^{app} \quad (4)$$

$$\Delta H^0 = [(2.303RT_1T_2)/(T_2 - T_1)] \times \log (K_{d1}^{app}/K_{d2}^{app}) \quad (5)$$

and

$$T\,\Delta S^0 = \Delta H^0 - \Delta G^0 \quad (6)$$

where R is the gas constant (1.986 cal/K · mol or 8.3166 J/K · mol), T the absolute temperature, ΔH^0 the standard enthalpy change and ΔS^0 the entropy change. ΔH^0 can be calculated from the slope of the van 't Hoff plot, with log K_d^{app} on the ordinate and $1/T$ on the abscissa, as shown in Fig. 3.

3. Application of affinity electrophoresis

3.1. Calculation of thermodynamic parameters of hydrophobic and hydrophilic interactions

3.1.1. Interaction between concanavalin A and carbohydrates

The dissociation constant of concanavalin A (Con A)–carbohydrate interactions were reported by Hořejší et al. [19] and Takeo et al. [20]. Takeo et al. reported that the dissociation constants of Con A for glycogen (K_d^{app}) and for the maltose type of oligosaccharide (K_i) [20] were almost equal to the dissociation constant for maltose regardless of the number of glucosyl residues. This indicates that the carbohydrate binding site of Con A appears to be one glucose unit.

In Fig. 1, the affinity patterns of the Con A–dextran interaction at (A) 22 and (B) 50°C are presented. The mobility of Con A decreases in the gel containing dextran. The higher the concentration of dextran, the stronger is the mobility decrease. The rate of this mobility decrease becomes less when the electrophoresis is carried out at higher temperature. Thus, at 22°C Con A in the presence of 0.5% dextran migrates about one quarter of the distance in the absence of dectran, whereas at 50°C the factor is about two thirds. As R_c of the Con A–dextran T-2000 complex should be zero, Eq. 2 is applicable. In Fig. 2, the affinity plots at various temperatures are illustrated. They all give straight lines and K_d^{app} was calculated to be 0.39, 0.66, 0.95, 1.35, 2.12 and 3.83 mM at 11, 22, 30, 39, 50 and 59°C, respectively. Thus, K_d^{app} increases about tenfold when the temperature increases by 48°C from 11 to 59°C. In other words, the affinity of Con A to dextran decreases to about one tenth when the temperature increases by 48°C. In Fig. 3A, the van 't Hoff plot for this Con A–dextran interaction is illustrated. The plot is straight in the temperature range between 10 and 50°C. Fig. 3B and C shows the van 't Hoff plots for the interactions of Con A with various monosaccharides and their glycosides and with maltose oligosaccharides, respectively. From the slope of the line, or with Eq. 5, ΔH^0 values are calculated. The entropy changes, ΔS^0, at 20°C were calculated with Eq. 6.

In Table 1, thermodynamic parameters of the interactions between Con A and various carbohydrates [16] are summarized. All Con A–carbohydrate interactions give negative entropy changes. The values coincide well with those obtained by equilibrium dialysis [21] and substitution titration of fluorescence quenching [22] using methylumbelliferyl-α-D-mannoside as an affinity ligand.

3.1.2. Interaction between glycogen phosphorylase and glycogen

Suzuki [23] reported the thermodynamic parameters of the interaction between rabbit skeletal muscle glycogen phosphorylase and glycogen. Electrophoresis was performed using the modified Davis [24] and Ornstein [25] buffer system, in which the separation gels were prepared with the buffer (pH 6.7) for the stacking gel preparation. With this buffer system, the pH

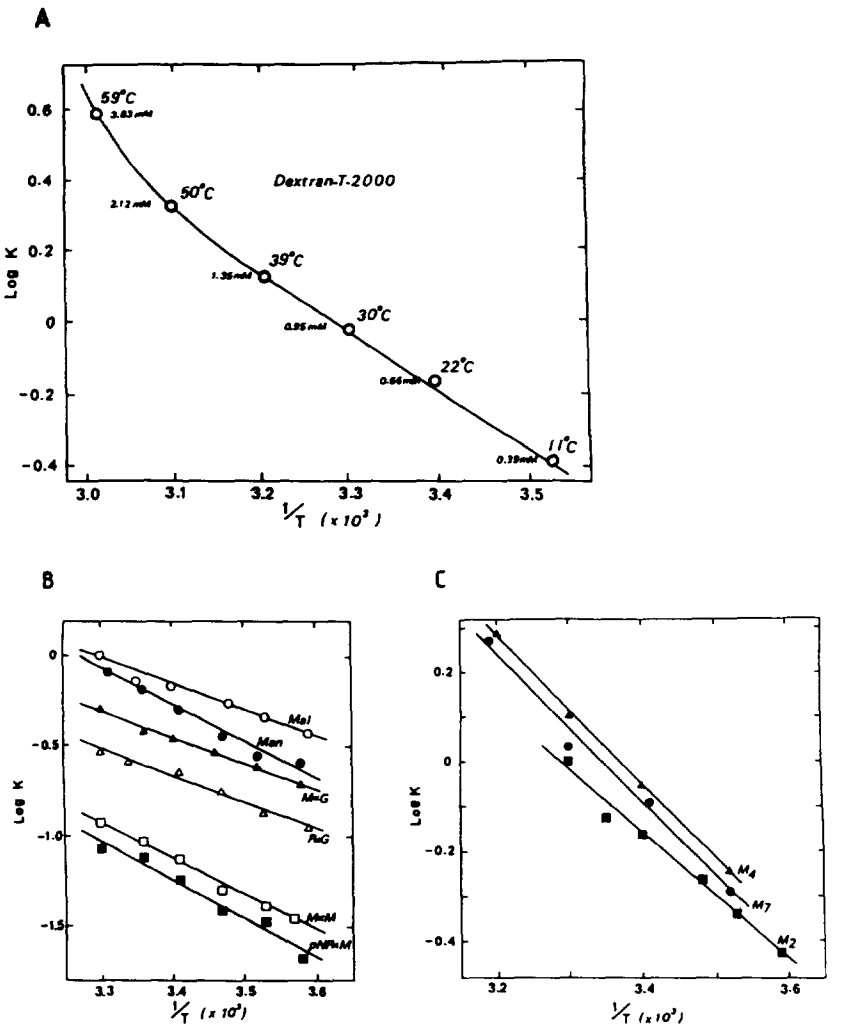

Fig. 3. Van 't Hoff plots for concanavalin A–carbohydrate interactions (Ref. [16]). (A) Con A–dextran interaction. A Van 't Hoff plot was prepared with the results from the affinity plots in Fig. 2. (B) Con A interaction with monosaccharides and their glycosides. Mal = Maltose; Man = D-mannose; MαG = methyl α-D-glucoside; PαG = phenyl α-D-glucoside; MαM = methyl α-D-mannoside; *p*NPαM = *p*-nitrophenyl-α-D-mannoside. (C) Con A interaction with maltose oligosaccharides. M_2 = Maltose; M_4 = maltotetraose; M_7 = maltoheptaose.

of the separation gel does not become higher than pH 8.6, whereas with the use of the original Davis–Ornstein buffer system, the pH becomes 9.5 during electrophoresis. At this alkaline pH, phosphorylase is unstable.

In Fig. 4, affinity plots for the interactions of phosphorylase *a* (P1-*a*) and *b* (P1-*b*) with glycogen at various temperatures are illustrated. Fig. 4A, B, C, D, E and F show the plots obtained at 5.0, 12.5, 20.0, 27.5, 35.0 and 42.5°C, respectively. The affinity plots of both phosphorylase forms and their temperature dependence are almost identical. All the plots give straight lines and both lines for P1-*a* and P1-*b* intercept the abscissa at the same point. The affinity of the phosphorylases decreases about 500-fold when the temperature increases by 37.5°C from 5 to 42.5°C. In Fig. 5, the Van 't Hoff plots for (A) P1-*b* and (B) P1-*a* are illustrated. The plots for both phosphorylases are

Table 1
Thermodynamic parameters for interactions between concanavalin A and carbohydrates (from Ref. [16])

Carbohydrate	K_d^{app} or K_i at 20°C (mM)	ΔG^0 (kcal/mol)	ΔH^0 (kcal/mol)	ΔS^0 (cal/mol · K)
Dextran T-2000	0.55	−4.3	−6.2	−6.3
Glycogen	0.81	−4.1	−11.0	−23.4
Maltose (M_2)	0.69	−4.2	−6.1	−6.4
	0.75[a]			
Maltotetraose (M_4)	0.89	−4.1	−7.5	−11.4
Maltoheptaose (M_7)	0.83	−4.1	−7.5	−11.3
M-α-G	0.32	−4.7	−6.2	−5.2
P-α-G	0.23	−4.9	−6.7	−6.3
M-α-M	0.074	−5.5	−9.4	−13.4
	0.156[b]	−5.18[b]	−9.07[b]	−13.37[b]
*p*NP-α-M	0.057	−5.7	−8.9	−10.9

[a] Bessler et al. [21], pH 7.0 at 27°C.
[b] Van Landschoot et al. [22], pH 5.5 at 25.3°C.

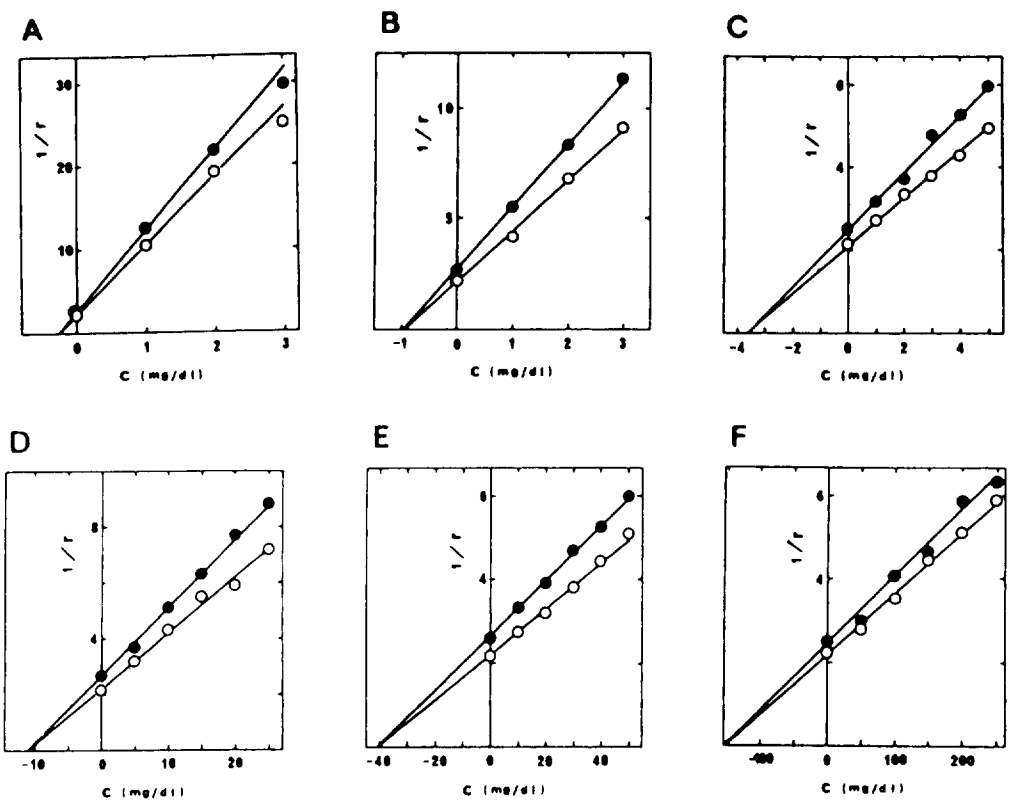

Fig. 4. Affinity plots of interactions between rabbit skeletal muscle glycogen phosphorylase and shell fish glycogen at various temperatures, drawn according to Eq. 2 (from Ref. [23]). (A), (B), (C), (D), (E) and (F) obtained at 5.0, 12.5, 20.0, 27.5, 35.0 and 42.5°C, respectively. ● = Phosphorylase *b*; ○ = phosphorylase *a*.

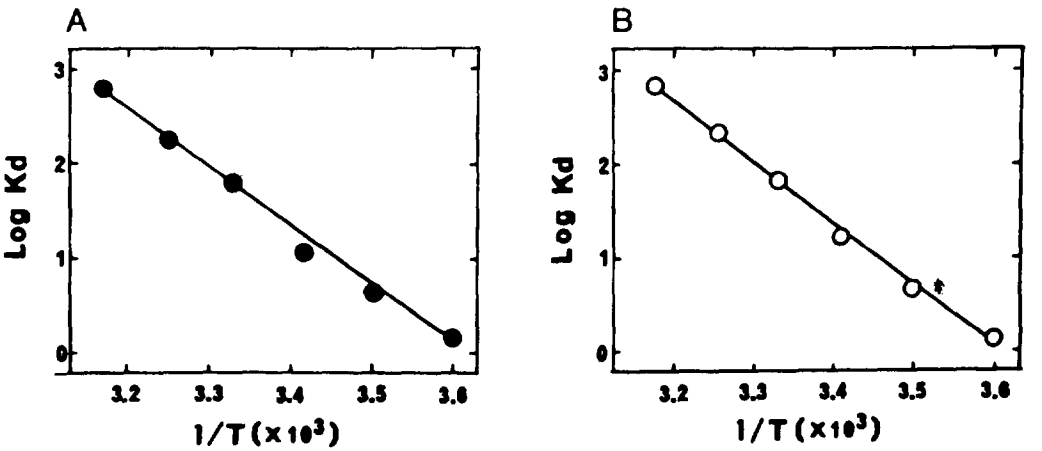

Fig. 5. Van 't Hoff plots of phosphorylase–glycogen interactions (from Ref. [23]). The plots were prepared with the results from the affinity plots in Fig. 4. (A) For phosphorylase *b*; (B) for phosphorylase *a*.

almost identical. In Table 2, thermodynamic parameters for P1-*b*–glycogen interaction are summarized. The entrophy change of the phosphorylase–glycogen interaction is negative, similarly to that for the Con A–dextran interaction.

3.1.3. Interactions between MOPC-315 myeloma protein and haptens

MOPC-315 myeloma protein is an IgA type of mouse immunoglobulin, which carries binding activity to dinitrophenyl (DNP) and trinitrophenyl (TNP) groups as a hapten. Tanaka et al. [26] reported the effect of temperature on the interaction between the immunoglobulin and the haptens. Electrophoresis was performed using the Davis [24] and Ornstein [25] buffer system. DNP and TNP ligands are prepared as their conjugates with acrylamide–allylamine copolymers, as reported in Section 3.2. In Fig. 6, affinity plots for the interaction of MOPC-315 monomer with TNP ligand at various temperatures are illustrated. K_d^{app} was calculated according to Eq. 2. In Table 3, K_d^{app} values for the

Table 2
Thermodynamic parameters for interaction between phosphorylase *b* and glycogen (from Ref. [23])

K_d^{app} at 20°C (μM)[a]	ΔG^0 at 20°C (kcal/mol)	ΔH^0 (kcal/mol)	ΔS^0 (cal/mol · K)
17.4	−6.4	−29.1	−77.7

[a] The molar concentration of glycogen was calculated by assuming that 1 g/dl is equivalent to 5 m*M* [3].

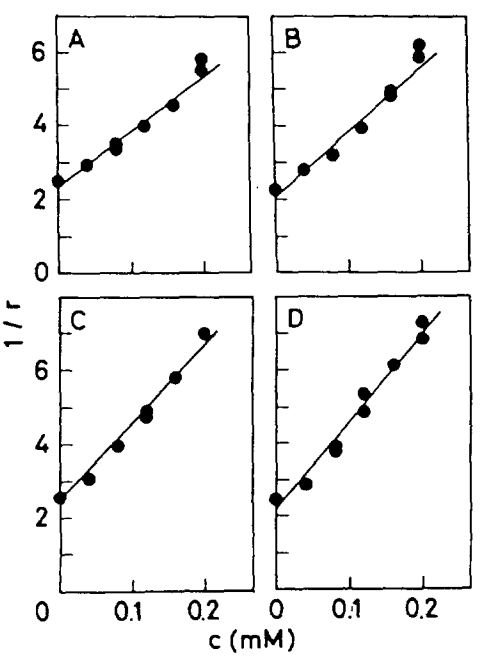

Fig. 6. Affinity plots of interactions between MOPC-315 monomer and TNP ligand, drawn according to Eq. 2 (from Ref. [26]). (A), (B), (C) and (D) obtained at 7, 20, 30 and 40°C, respectively.

Table 3
Apparent dissociation constant (K_d^{app}) of interactions between MOPC 315 myeloma protein and TNP or DNP affinity ligand at various temperatures (from Ref. [26])

MOPC-315	Affinity ligand	K_d^{app} (mM)				
		7°C	20°C	30°C	40°C	50°C
Monomer	TNP	0.15	0.11	0.11	0.086	–
Monomer	DNP	4.6	2.8	2.2	1.7	–
Dimer	DNP	2.0	0.83	0.56	0.33	–
Fab' fragment	TNP	0.42	0.30	0.25	0.26	3.6
Fab' fragment	DNP	–	4.6	–	–	–

interactions between monomeric and dimeric forms and the Fab' fragment and DNP and TNP haptens at various temperatures are summarized. Every form of the myeloma protein shows a higher affinity to the TNP than to the DNP ligand. Their affinity to those haptens becomes stronger with increasing temperature, in contrast to the phosphorylase–glycogen interaction. K_d^{app} for the Fab' fragment–TNP ligand interaction at 7°C, for instance, is $0.42 \cdot 10^{-3}$ M, whereas at 40°C it is $0.26 \cdot 10^{-3}$ M. In other words, the affinity of the Fab' fragment of MOPC-315 myeloma protein to TNP-hapten is doubled when the temperature increases by 33°C from 7 to 40°C. At 50°C, its affinity decreased abruptly. The affinity electrophoresis pattern obtained at 50°C shows a new band, which is assumed to be a light chain dimer [27] because of its low affinity to DNP-hapten and its migration position.

In Table 4, thermodynamic parameters of the MOPC-315 myeloma protein interactions are summarized. In Fig. 7, the Van 't Hoff plots for the interactions between MOPC-315 monomer and its Fab' fragment and DNP and TNP ligands

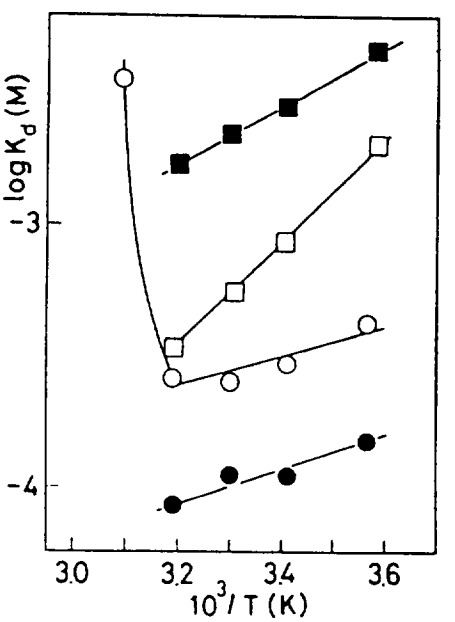

Fig. 7. Van 't Hoff plots of interactions between MOPC 315 or its Fab' fragment and DNP or TNP ligand (Ref. [26]). ■ = Interaction between MOPC 315 monomer and DNP ligand; □ = MOPC 315 dimer and DNP ligand; ○ = MOPC 315 Fab' fragment and TNP ligand; ● = MOPC 315 monomer and TNP ligand.

Table 4
Thermodynamic parameters of interactions between MOPC-315 myeloma protein and TNP or DNP affinity ligand (Ref. [26])

MOPC-315	Affinity ligand	ΔG^0 (kcal/mol)	ΔH^0 (kcal/mol)	ΔS^0 (cal/mol · K)
Monomer	TNP	−5.3	2.8	28
Monomer	DNP	−3.4	5.2	29
Dimer	DNP	−4.1	9.2	46
Fab' fragment	TNP	−4.7	2.8	26

are illustrated. Each plot gives a straight line within the temperature range 7–40°C. Their ΔH^0 and ΔS^0 values are positive, in contrast to the Con A–dextran or phosphorylase–glycogen interaction.

3.1.4. *Interaction between fibronectin and gelatin*

Fibronectin is a high-molecular-mass, multiple-domain glycoprotein, which is found in a soluble form in plasma and other body fluids. It binds to collagen, but better to denatured collagen or gelatin than to native collagen. One of the biological functions of the fibronectin binding to gelatin is considered to be mediation of reticuloendothelial or macrophage clearance of collagen debris and that of fibrin microaggregates [28]. Kashiwagi and co-workers [29,30] first applied affinity electrophoresis to analyse the fibronectin–gelatin interaction.

Electrophoresis was performed using the Davis–Ornstein [24,25] buffer system. Because the affinity of fibronectin to gelatin is too high to estimate the exact affinity constant, the separation and stacking gels are prepared in the presence of 3 *M* urea. In Fig. 8, affinity plots for the fibronectin–gelatin interaction at various temperatures are illustrated. The lower the temperature, the stronger is the affinity, as observed for the Con A–dextran interaction. Thus, the affinity at 15°C is 230 times stronger than that at 50°C. The results coincide well with the report of Hörmann and Jilek [31], who analysed the interaction by means of enzyme-linked immuno-

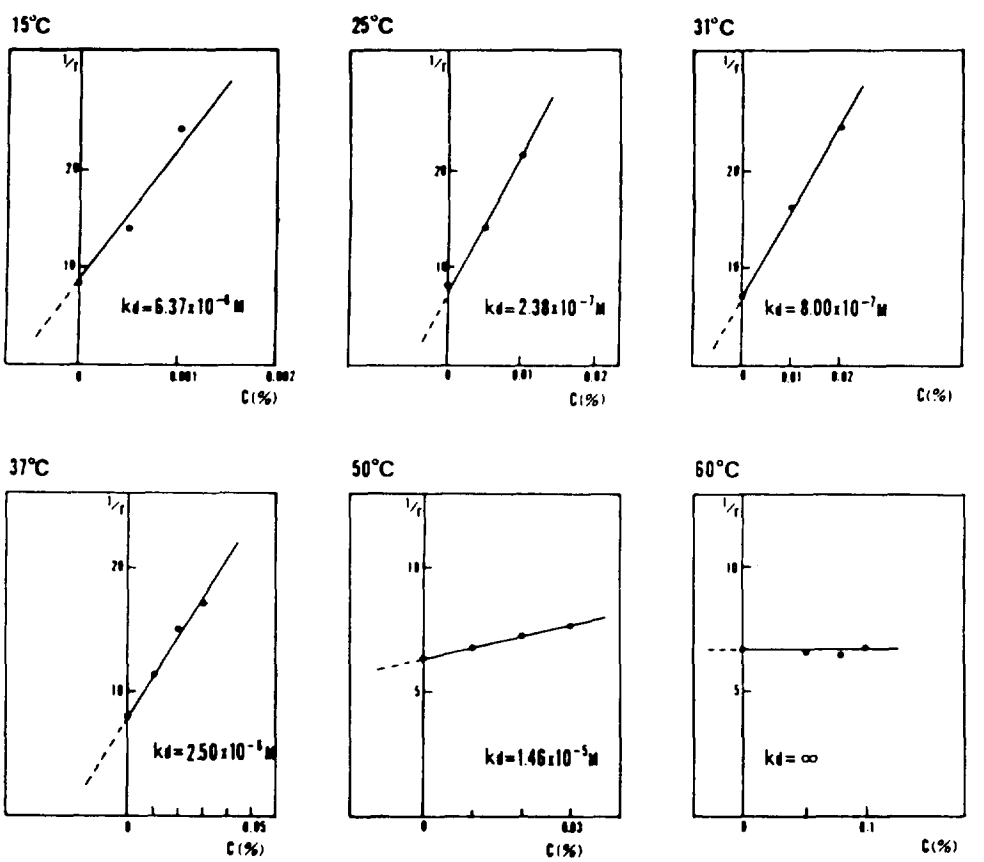

Fig. 8. Affinity plots of interaction between human serum fibronectin and bovine bone gelatin at various temperatures (from Ref. [29]). The plots were drawn according to Eq. 2. K_d^{app}: $6.37 \cdot 10^{-8}$ *M* at 15°C, $2.36 \cdot 10^{-7}$ *M* at 25°C, $8.0 \cdot 10^{-7}$ *M* at 31°C, $2.5 \cdot 10^{-6}$ *M* at 37°C and $1.46 \cdot 10^{-5}$ *M* at 50°C.

sorbent assay. They reported that the binding of fibronectin to collagen was stronger at lower temperatures. In Fig. 9, the Van 't Hoff plot is illustrated. It gives a good straight line between 15 and 50°C. ΔH^0 and ΔS° at 37°C are both negative and calculated to be −29.9 kcal/mol and −70.5 cal/K · mol, respectively.

3.1.5. Temperature dependence of hydrophilic and hydrophobic interaction

In Fig. 10, the Van 't Hoff plots of the above-mentioned interactions are rearranged. In general, it is considered that hydrophobic interactions are entropy-increasing reactions, because of the loss of the binding water on the surface of the hydrophobic group of the interacting molecules on complex formation. In fact, the interaction between MOPC-315 and DNP or TNP ligand enhanced their affinity at increasing temperature and their Van 't Hoff plots give positive slopes, as indicated in Fig. 10, line C. The calculated entropy change is positive. In contrast, the affinity of Con A–dextran and phosphorylase–glycogen interactions increases with decreasing temperature and their Van 't Hoff plots give negative slopes, as indicated in Fig. 10, lines A and B. The calculated entropy changes of both hydrophilic interactions are negative. Matsumoto et al. [32] reported that the Van 't Hoff plot for a branching enzyme–glycogen interaction also gives a negative slope and a negative ΔS^0.

With regard to the fibronectin–collagen interaction, the affinity increases with decreasing temperature, as seen for the hydrophilic interactions such as the Con A–dextran interaction. The Van 't Hoff plot also gives a negative slope, as indicated in Fig. 10, line D. These results indicate that the fibronectin–collagen interaction can be assumed to be hydrophilic.

Forastieri and Ingham [33] studied the interaction thermodynamically using fluorescein-conjugated fibronection. They suggested that the

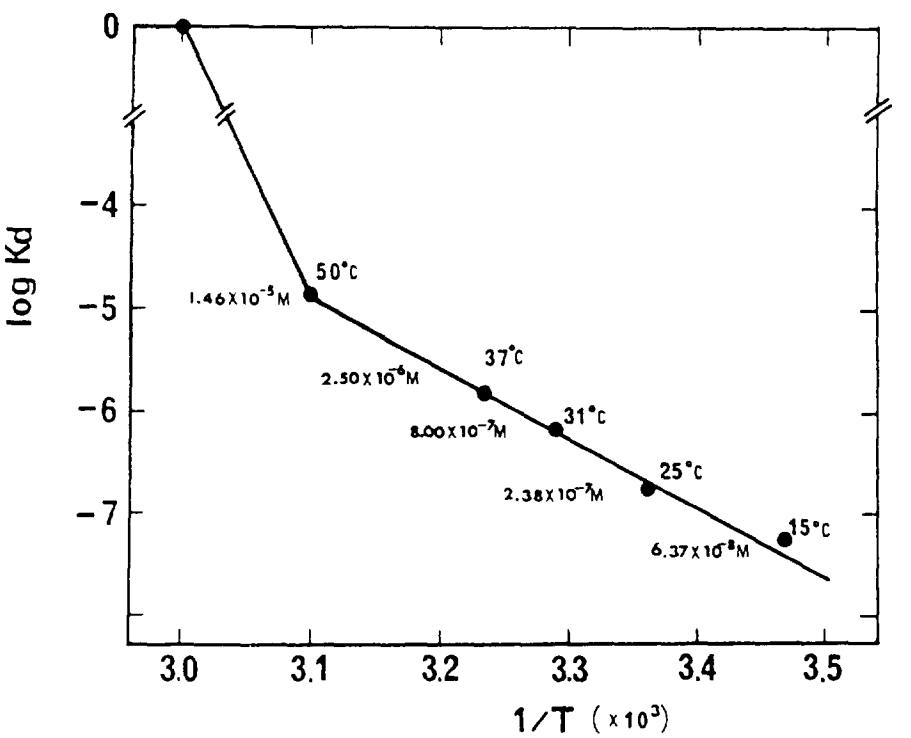

Fig. 9. Van 't Hoff plot of fibronectin–gelatin interaction (from Ref. [29]). The plot was prepared with results from the affinity plots in Fig. 8.

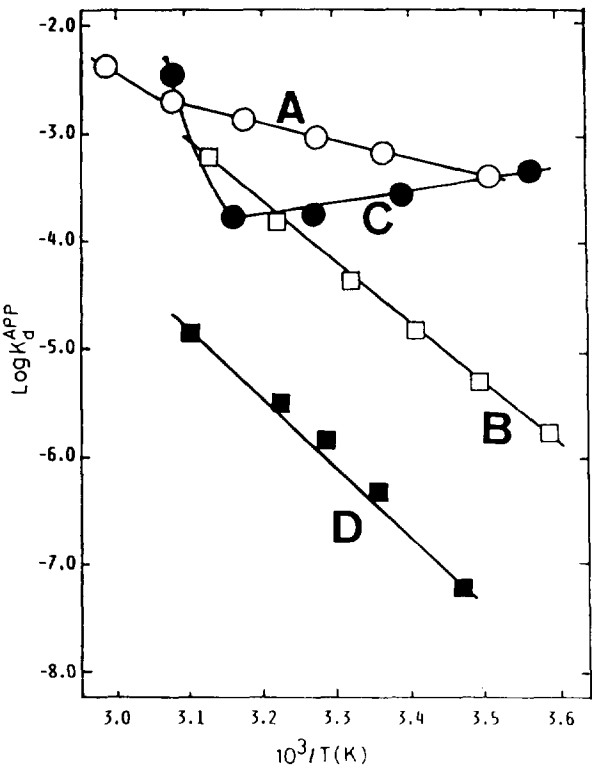

Fig. 10. Van 't Hoff plots of various biospecific interactions. (A) Concanavalin A–dextran; (B) glycogen phosphorylase *b*–glycogen; (C) MOPC 315 Fab' fragment–TNP ligand; (D) fibronectin–gelatin interactions.

interaction appears not to be hydrophobic. As the affinity of the fibronectin–collagen interaction abruptly decreases on addition of urea, it is considered that hydrogen bonding plays a decisive role on the fibronectin–collagen interaction.

In conclusion, when an accurately controlled thermostated polyacrylamide gel disc electrophoresis apparatus is available, affinity electrophoresis offers a simple and convenient method for calculating the thermodynamic parameters of biospecific interactions. Thus, biospecific interactions seem to be thermodynamically formulated into two types: (1) hydrophilic interactions such as those between Con A and dectran or glycogen phosphorylase and glycogen; in these interactions, their affinity decreases with a rise in temperature and $\Delta H°$ and $\Delta S°$ are negative; (2) in contrast, in hydrophobic interactions such as those between MOPC-315 myeloma protein and DNP- or TNP-hapten, the affinity increases with increase in temperature; in these interactions, ΔH^0 and ΔS^0 are calculated to be positive.

3.2. Development of two-dimensional affinity electrophoresis

3.2.1. Complete separation of anti-hapten antibodies

Induced antibodies against a single antigenic determinant are highly heterogeneous. Two-dimensional electrophoresis, based first on the diversity of electric charge and second on differences in binding activity, should be efficient for separating heterogeneous protein mixtures of equal molecular mass such as immunoglobulin. On this bases, Takeo et al. [34] developed a new type of two-dimensional electrophoresis, utilizing capillary polyacrylamide gel isoelectric focusing (PAG-IEF: 85 mm high × 12 mm diameter) in the first direction and slab PAG affinity electrophoresis (inner space 100 mm high × 85 mm wide × 1 mm thick) in the second direction. They called it two-dimensional affinity electrophoresis (2D-AEP). In practice, the affinity electrophoresis in the second direction is carried out with the use of a buffer system with double the concentration of the original buffer system reported by Reisfeld et al. [35]. Heegaard [36] reported the dependence of the affinity of IgG on the ionic strength of the buffer system. When electrophoresis is carried out with the use of a discontinuous buffer system, maintenance of its salt concentration should be taken in consideration.

Hapten-conjugated non-cross-linked acrylamine–allylamine copolymers are used as macromolecular affinity ligands. A non-cross-linked copolymer of acrylamide and allylamine (10:1, w/w) was conjugated with one of the aromatic haptenic groups at the position of amine groups of the copolymer using dinitrofluorobenzene, trinitrobenzene sulphonate or dansyl chloride. The synthesized conjugates of DNP, TNP and dansyl groups with acrylamide–allylamine co-

polymer, DNP–PA, TNP–PA and dansyl–PA, were used as macromolecular affinity ligands for analysing anti-DNP, anti-TNP or anti-dansyl antibodies, respectively. Dextran T-2000 and fluorescein isothiocyanate (FITC)-conjugated dextran T-2000 are used as macromolecular affinity ligands for affinity electrophoresis of anti-dextran and anti-fluorescein isothiocyanate antibodies, respectively.

In Fig. 11, the two-dimensional affinity pattern of one of the rabbit anti-DNP antibodies (1Z-4) [37], which was purified by affinity chromatography on a DNP-Sepharose column, is presented. PAG-IEF was carried out with a capillary gel (T = 5%, C = 3%; carrier ampholyte: pH 4–9, 1.25%; pH 5–8, 1.25%) and affinity electrophoresis with the modified buffer system reported by Reisfeld et al. [35], using the separation gel (T = 5.13%, C = 2.59%), containing 250 μM DNP-PA. The rabbit anti-DNP antibody was separated into several hundred IgG spots depending on the difference in their electric charge and affinity to the hapten. These spots are grouped into a number of families which are composed of several IgG spots having an identical affinity to the hapten but different p*I* values. As shown in Fig. 11, clearly separated IgG families are designated families a–u.

3.2.2. *Cross-reactivity of anti-hapten antibodies*

In Fig. 12A, the 2D-AEP pattern of one of the rabbit anti-dansyl antibodies with use of a separation gel containing 100 μM dansyl-PA [38] is presented. This anti-dansyl antibody is separated into several hundred IgG spots and they can be grouped into IgG families which are composed of several IgG spots having the same affinity to the hapten but different p*I*s, as in the case of the anti-DNP antibody. Nakamura and co-workers reported that mouse anti-FITC antibodies [39] and mouse anti-DNP antibodies [40] are also separated in the same manner.

In order to detect cross-reactivity of the antibody, the same anti-dansyl antibody as shown in Fig. 12A is applied to 2D-AEP in the presence of heterologous haptenic ligands, DNP-PA. In Fig. 12B, the 2D-AEP pattern in the presence of 1 mM DNP-PA is shown. The majority of the IgG spots or IgG families exhibit no affinity to DNP-hapten. However, a few families, e.g., a, b, c and d, show mobility changes, indicating cross-reactivity to heterologous DNP-hapten.

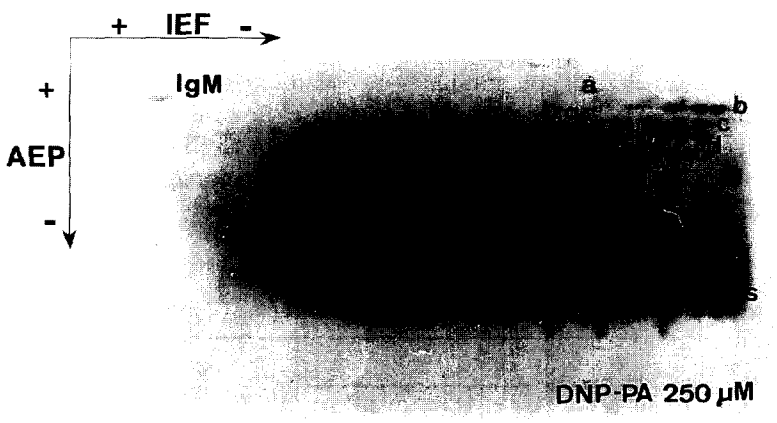

Fig. 11. Two-dimensional affinity electrophoresis pattern of a rabbit anti-DNP antibody (1Z-4) (from Ref. [37]). First direction, capillary polyacrylamide gel isoelectric focusing (IEF); second direction, affinity electrophoresis (AEP) in the presence of 250 μM DNP–PA. Antibody spots were detected on the electroblotted nitrocellulose membrane by immunochemical fixation and peroxidase activity staining. IgM spot was detected in the corner of the gel and the IgG class of the antibody was spread over the entire gel. Clearly separated IgG spots are grouped into IgG families, designated a–u.

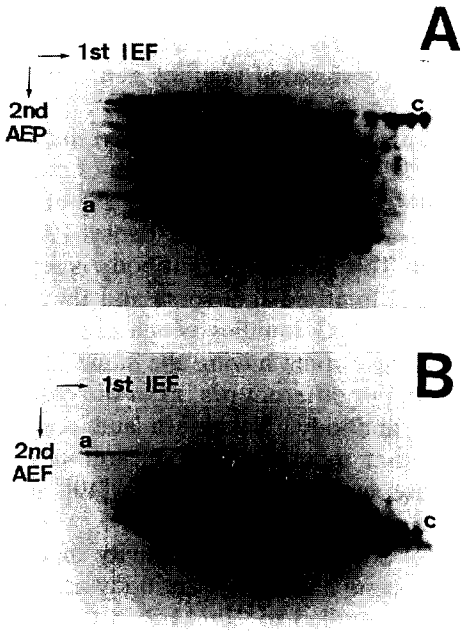

Fig. 12. Two-dimensional affinity electrophoresis patterns of a rabbit anti-dansyl antibody in the presence of (A) homologous and (B) heterologous hapten (from Ref. [38]). (A) 2D-AEP pattern in the presence of 0.1 m*M* dansyl-PA; (B) in the presence of 1 m*M* DPN-PA.

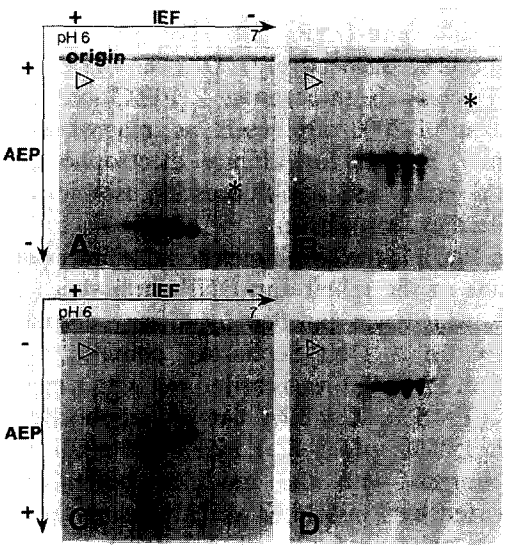

Fig. 13. Two-dimensional affinity electrophoresis patterns of mouse monoclonal antibody 35.8.2H (IgG_1, BALB/c) (from Ref. [41]). (A) and (B) 2D-AEP patterns obtained by the Reisfeld et al. [35] buffer system (pH 3.8) (A) in the absence and (B) in the presence of $4.0 \cdot 10^{-3}$ g/ml dextran B512. (C) and (D) 2D-AEP patterns of the same antibody obtained using the Davis [24] and Ornstein [25] buffer system at pH 9.5 (C) in the absence and (D) in the presence of $6.5 \cdot 10^{-6}$ g/ml dextran B512.

From the affinity pattern, K_d^{app} of the anti-dansyl IgG families to dansyl- and DNP-hapten have been calculated. The results are summarized in Table 5. It is interesting that whereas families b, c and d show a stronger affinity to the homologous dansyl-hapten than to the heterologous DNP-hapten, family a shows a stronger affinity to the heterologous hapten. The authors could not find cross-reactivity in the reverse direction, namely cross-reactivity of anti-DNP antibodies against dansyl-hapten.

3.2.3. *Two-dimensional affinity pattern of monoclonal antibody*

Mimura et al. [41] subjected dectran-specific mouse hybridoma antibody (35.8.2H; IgG_1, BALB/c) to 2D-AEP. As illustrated in Fig. 13, this monoclonal antibody was separated into about six spots which had an affinity identical

Table 5
Cross-reactivity of anti-dansyl antibody and its K_d^{app} to dansyl- and DNP-hapten (Ref. [38])

Anti-dansyl IgG family	K_d^{app} for		Affinity ratio (B/A)
	(A) Dansyl ($\times 10^{-4}$ *M*)	(B) DNP ($\times 10^{-3}$ *M*)	
a	4.77	0.296	0.62
b	0.846	0.364	4.30
c	0.276	1.47	53.4
d	0.353	0.161	4.55

with dectran B512, but with different p*I* values. As the affinity pattern of the monoclonal antibody is very similar to each family of anti-hapten antibodies, the authors assumed that each family of anti-hapten antibodies is derived from a single clone of antibody-producing cell line. The results obtained from the studies on cross-reactivity of anti-dansyl antibodies mentioned above give further support to the assumption. The authors obtained no experimental proof regarding the origin of the microheterogeneity of each IgG family of the induced antibody preparations and of monoclonal antibodies. Some post-translational modification of the immunoglobulin molecule could be postulated for the microheterogeneity, possibly different stages of processing of sugar chains or deamidation of the peptide chain of the immunoglobulin molecule.

The high resolving power of 2D-AEP provides a powerful tool to solve fundamental problems of immunochemistry, such as the analysis of antibody heterogeneity, quantitative evaluation of the diversity of antigen-binding activity and cross-reactivity of each immunoglobulin family of induced antibodies, antigen-dependent somatic mutation and immunotolerance and the preparation of monoclonal antibodies from a polyclonal antibody.

3.3. Lectin affinity electrophoresis

Specific interactions between lectin and serum glycoproteins were first investigated by electrophoresis 1960 by Nakamura et al. [42]. They demonstrated strong mobility changes of α-, β- and γ-globulin fractions at the crossing points of serum protein with concavalin A in two-dimensional cross-electrophoresis [43]. In 1973, Bøg-Hansen [5] developed a highly sensitive separation method for individual serum glycoproteins using the specific interaction of glycoproteins with concanavalin A in crossed immunoelectrophoresis [44]. He detected the presence of microheterogeneity in various serum glycoprotein components. He designated the method crossed affinity immunoelectrophoresis. In 1980, Bøg-Hansen and Takeo [17] reported K_d^{app} values for eight human serum glycoprotein fractions with the use of the crossed affinity electrophoresis, such as orosomucoids and antitrypsins. In 1984, Rosalki and Foo [10] reported a simple method for the differentiation of bone and liver alkaline phosphatases with the use of cellulose acetate membrane electrophoresis and wheat germ agglutinin as the affinity ligand. They designated the method simply lectin affinity electrophoresis. In the same year, Taketa et al. [45] developed two-dimensional lectin affinity electrophoresis using two lectins having different carbohydrate binding specificies in a rectangular direction for differentiating human α-fetoproteins obtained from various pathological conditions. All these affinity electrophoreses, which utilize specific interactions of the lectin towards sample proteins, are designated lectin affinity electrophoresis.

The appearance of microheterogeneity of glycoproteins seems to result from different stages of post-translational processing of their prosthetic carbohydrate groups. Therefore, analysis of this microheterogeneity offers important information on cellular activity in the maturation process of glycoprotein-synthesizing cells and on their pathological conditions. As lectin affinity electrophoresis is easily manipulated and its principle is simply based on the binding specificity of lectins to carbohydrate, the technique is used widely for analysing the microheterogeneity of serum glycoproteins and enzymes. Thus, Taketa et al. [46] suggested a carbohydrate chain structure of α-fetoproteins from human cord serum and serum from patients with hepatocellular carcinoma based on the results obtained with lectin affinity electrophoresis. Kobata and Endo [47] proposed a complete separation procedure for oligosaccharides and glycopeptides with the systematic use of immobilized lectin columns. Lee et al. [48] analysed the binding specificity of carbohydrates to concanavalin A with the use of fluorescent conjugates of oligosaccharides. Although chemical analysis of the carbohydrate chain structure can provide conclusive evidence for the carbohydrate structure of glycoproteins, the procedure is complicated. On the other hand, lectin affinity electrophoresis is

simple and offers a convenient technique for characterizing glycoproteins.

3.4. Capillary gel affinity electrophoresis

Capillary electrophoresis [49–52] is a newly developed separation technique, derived from the combination of the principles of electrophoresis with high-performance liquid chromatography. Its high resolving power and automatic operation system make it an important separation technique in biochemistry.

Application of the affinity technique to capillary electrophoresis should give a useful approach for characterizing biospecific interactions. Thus, Guttman and Cooke [53] reported a high resolution of DNA restriction fragments by capillary gel affinity electrophoresis by adding ethidium bromide as an affinity ligand to the polyacrylamide gel. Its efficiency is much superior to that of capillary electrophoresis. They evaluated its separation efficiency as high as 10^7 theoretical plates per metre. Chu et al. [54] determined binding constants of aryl sulfonamides to bovine carbonic anhydrase B with the use of capillary gel affinity electrophoresis. They discussed the convenience of this method in comparison with affinity gel electrophoresis. Although affinity gel electrophoresis is generally useful and convenient for determining binding constants of macromolecular interactions, particularly when only small amounts are available, capillary gel affinity electrophoresis is convenient for determining binding constants of proteins to low-molecular-mass ligands. Automation of the operating procedure and of the calculation of the kinetic constants makes capillary gel affinity electrophoresis more useful in biochemical and clinical fields.

Acknowledgements

I am indebted to the following staff members and research associates for their assistance and collaboration during the years of our research on affinity electrophoresis: Dr. Kazuyuki Nakamura, Dr. Tatehiko Tanaka, Dr. Yusuke Mimura, Dr. Ryosuke Suzuno, Mr. Masanori Fujimoto, Dr. Akira Kuwahara, Dr. Isao Suzuki and Dr. Shiro Kashiwagi.

References

[1] K. Takeo, *Adv. Electrophoresis*, 1 (1987) 229.
[2] K. Takeo and S. Nakamura, *Arch. Biochem. Biophys.*, 153 (1972) 1.
[3] C.F. Cori, G.T. Cori and A.A. Green, *J. Biol. Chem.*, 151 (1943) 39.
[4] K. Takeo and S. Nakamura, in O. Hoffmann-Ostenhof, M. Breitenbach, F. Koller, D. Kraft and O. Scheiner (Editors), *Affinity Chromatography*, Pergamon Press, Oxford, 1978, p. 67.
[5] T.C. Bøg-Hansen, *Anal. Biochem.*, 56 (1973) 480.
[6] V. Hořejší and J. Kocourek, *Biochim. Biophys. Acta*, 337 (1974) 338.
[7] M. Caron, A. Faure and P. Cornillot, *J. Chromatogr.*, 103 (1975) 160.
[8] S. Nakamura, K. Takeo, K. Tanaka and T. Ueta, *Hoppe-Seyler's Z. Physiol. Chem.*, 318 (1960) 115.
[9] K. Ek and P.G. Righetti, *Electrophoresis*, 1 (1980) 137.
[10] S.B. Rosalki and A.Y. Foo, *Clin. Chem.*, 30 (1984) 1182.
[11] K. Taketa, E. Ichikawa, H. Taga and H. Hirai, *Electrophoresis*, 6 (1985) 493.
[12] K. Takeo, *Electrophoresis*, 5 (1984) 187.
[13] V. Hořejší and M. Tichá, *J. Chromatogr.*, 376 (1986) 49.
[14] T.C. Bøg-Hansen, in W.H. Scouten (Editor), *Solid Phase Biochemistry. Analytical and Synthetic Aspects*, Wiley, New York, 1983, p. 223.
[15] K. Taketa, *J. Chromatogr.*, 569 (1991) 229.
[16] K. Takeo, *Lectins*, 2 (1982) 583.
[17] T.C. Bøg-Hansen and K. Takeo, *Electrophoresis*, 1 (1980) 67.
[18] N.H.H. Heegaard and O.T. Bjerrum, *Anal. Biochem.*, 195 (1991) 319.
[19] V. Hořejší, M. Tichá and J. Kocourek, *Biochim. Biophys. Acta*, 499 (1977) 290.
[20] K. Takeo, M. Fujimoto, A. Kuwahara, R. Suzuno and K. Nakamura, in R.C. Allen and P. Arnaud (Editors), *Electrophoresis '81*, Walter de Gruyter, Berlin, 1981, p. 33.
[21] W. Bessler, J.A. Shafer and I.J. Goldstein, *J. Biol. Chem.*, 249 (1974) 2819.
[22] A. Van Landeschoot, F.G. Loostiens and C.K. de Bruyne, *Eur. J. Biochem.*, 103 (1980) 307.
[23] I. Suzuki, *Yamaguchi-Igaku*, 34 (1985) 319.
[24] B.J. Davis, *Ann. N.Y. Acad. Sci.*, 121 (1964) 404.
[25] L. Ornstein, *Ann. N.Y. Acad. Sci.*, 121 (1964) 321.
[26] T. Tanaka, R. Suzuno, K. Nakamura, A. Kuwahara and K. Takeo, *Electrophoresis*, 7 (1986) 204.

[27] I. Schechter, E. Ziv and A. Licht, *Biochemistry*, 15 (1976) 2785.
[28] T.M. Saba and E. Jaffe, *Am. J. Med.*, 68 (1980) 577.
[29] S. Kashiwagi, K. Nakamura, K. Takeo, T. Takasago, A. Uchimichi and H. Ito, *Electrophoresis*, 12 (1991) 420.
[30] K. Nakamura, S. Kashiwage and K. Takeo, *J. Chromatogr.*, 597 (1992) 351.
[31] H. Hörmann and F. Jilek, *Artery*, 8 (1980) 482.
[32] A. Matsumoto, T. Nakajima and K. Matsuda, *J. Biochem.*, 107 (1990) 123.
[33] H. Forastieri and K.C. Ingham, *J. Biol. Chem.*, 260 (1985) 10546.
[34] K. Takeo, K. Nakamura and R. Suzuno, *J. Chromatogr.*, 597 (1992) 365.
[35] R.A. Reisfeld, U.J. Lewis and D.E. Williams, *Nature*, 195 (1962) 281.
[36] N.H.H. Heegaard, *Anal. Biochem.*, 208 (1993) 317.
[37] K. Takeo, R. Suzuno, T. Tanaka and K. Nakamura, *Electrophoresis*, 10 (1989) 813.
[38] K. Takeo, T. Tanaka, K. Nakamura and R. Suzuno, *Electrophoresis*, 10 (1989) 818.
[39] K. Nakamura, Y. Mimura and K. Takeo, *Electrophoresis*, 14 (1993) 81.
[40] K. Nakamura, Y. Mimura, T. Tanaka, Y. Fujikura and K. Takeo, *Electrophoresis*, 14 (1993) 1338.
[41] Y. Mimura, K. Nakamura and K. Takeo, *J. Chromatogr.*, 597 (1992) 345.
[42] S. Nakamura, K. Tanaka and S. Murakawa, *Nature*, 188 (1960) 144.
[43] S. Nakamura, *Cross Electrophoresis*, Igaku Shoin, Tokyo, and Elsevier, Amsterdam, 1966.
[44] P.J. Svendsen and N.H. Axelsen, *J. Immunol. Methods*, 1 (1972) 169.
[45] K. Taketa, E. Ichikawa, M. Izumi, H. Taga and H. Hirai, in V. Neuhoff (Editor), *Electrophoresis '84*, Verlag Chemie, Weinheim, 1984, p. 137.
[46] K. Taketa, Y. Fujii, Y. Aoi, H. Taga and S. Nishi, *Electrophoresis*, 14 (1993) 798.
[47] A. Kobata and T. Endo, *J. Chromatogr.*, 597 (1992) 111.
[48] K.B. Lee, Y.S. Kim and R.J. Linhardt, *Anal. Biochem.*, 203 (1992) 206.
[49] J.W. Jorgenson and K.D. Lukacs, *Science*, 222 (1983) 266.
[50] S. Hjertén and M.D. Zhu, *J. Chromatogr.*, 347 (1985) 191.
[51] R.A. Wallingford and A.G. Ewing, *Anal. Chem.*, 59 (1987) 1762.
[52] M.J. Gordon, X. Huang, S.L. Pentoney, Jr., and R.N. Zare, *Science*, 242 (1988) 224.
[53] A. Guttman and N. Cooke, *Anal. Chem.*, 63 (1991) 2038.
[54] Y.-H. Chu, J.K. Chen and G.M. Whitesides, *Anal. Chem.*, 65 (1993) 1314.